



Climate deterioration in the Eastern Mediterranean as revealed by ion microprobe analysis of a speleothem that grew from 2.2 to 0.9 ka in Soreq Cave, Israel

Ian J. Orland^{a,*}, Miryam Bar-Matthews^b, Noriko T. Kita^a, Avner Ayalon^b, Alan Matthews^c, John W. Valley^a

^a Department of Geology and Geophysics, University of Wisconsin, 1215 W Dayton Street, Madison, WI, 53706, USA

^b Geological Survey of Israel, 30 Malchei Israel Street, Jerusalem, 95501, Israel

^c The Institute of Earth Sciences, The Hebrew University, Givat Ram, Jerusalem, 91904, Israel

ARTICLE INFO

Article history:

Received 11 October 2007

Available online 25 October 2008

Keywords:

Paleoclimate

Speleothem

Oxygen isotopes

Ion microprobe

Confocal laser fluorescent microscopy

Eastern Mediterranean

ABSTRACT

Analysis of oxygen isotope ratios ($\delta^{18}\text{O}$) by ion microprobe resolves a sub-annual climate record for the Eastern Mediterranean from a Soreq Cave stalagmite that grew between 2.2 and 0.9 ka. In contrast to conventional drill-sampling methods that yield a total variation of 1.0‰ in $\delta^{18}\text{O}_{\text{calcite}}$ values across our sample, the methods described here reveal up to 2.15‰ variation within single annual growth bands. Values of $\delta^{18}\text{O}$ measured by ion microprobe vary in a regular saw-tooth pattern that correlates with annual, fluorescent growth banding where calcite grades from light to dark fluorescence. Modern records of precipitation and of cave dripwater indicate that variable $\delta^{18}\text{O}_{\text{calcite}}$ values record regular seasonal differences in $\delta^{18}\text{O}_{\text{rainfall}}$ modified by mixing in the vadose zone. Large differences in $\delta^{18}\text{O}$ values measured across a single band (i.e., between the dark and light fluorescent calcite, or $\Delta^{18}\text{O}_{\text{dark-light}}$) are interpreted to indicate wetter years, while smaller differences represent drier years. Oxygen isotopes record: 1) month-scale growth increments, 2) changes in $\Delta^{18}\text{O}_{\text{dark-light}}$ that represent seasonality, 3) a systematic, long-term decrease in maximum $\Delta^{18}\text{O}_{\text{dark-light}}$ values, and 4) an overall increase in average $\delta^{18}\text{O}_{\text{calcite}}$ values through time. These results suggest a drying of regional climate that coincides with the decline of the Roman and Byzantine Empires in the Levant region.

© 2008 University of Washington. All rights reserved.

Introduction

Soreq Cave, Israel, contains a record of continuous cave-deposit (speleothem) growth from 185 ka to the present, and these speleothems are the focus of many paleoclimate investigations (Bar-Matthews et al., 1996, 1997, 2003; Ayalon et al., 1999; Matthews et al., 2000; Kolodny et al., 2003; McGarry et al., 2004). Speleothems in Soreq Cave preserve geochemical signals of local climate as they grow. If calcite is precipitated in isotopic equilibrium, oxygen isotopes in speleothem calcite can provide a geochemical measure of past climate change (Hendy, 1971). At decadal to century scales, fluctuations in the $\delta^{18}\text{O}$ values preserved in Soreq Cave speleothems reflect changes in rainfall amount, the rainfall source, and cave-air temperature. It follows that on annual or sub-annual time scales $\delta^{18}\text{O}_{\text{calcite}}$ measurements may reveal records of seasonality as well as paleoclimate. Hence, the goal of this study is to improve the temporal resolution of the Soreq Cave oxygen isotope record by using an ion microprobe to acquire high spatial-resolution $\delta^{18}\text{O}$ analyses.

Crucial for this study is the body of previous work that characterizes modern Soreq Cave conditions, local climate patterns, and cave hydrology (Ayalon et al., 1998, 2004; Kaufman et al., 2003). These studies chronicle multiple climatic and geochemical variables,

including surface and cave-air temperature, rainfall amount and isotopic composition, dripwater chemistry, and cave atmosphere composition. Significantly, there is a regular pattern of seasonal variation in regional climate; on average, 95% of the annual precipitation falls during the winter “wet season” between November and April, with January being the wettest month (Fig. 1; Ayalon et al., 2004; Mitchell and Jones, 2005). These records also show that the $\delta^{18}\text{O}$ values of averaged monthly rainfall are highest at the beginning and end of each wet season, and lowest during the periods of increased precipitation (Fig. 1). Barring substantial mixing of seasonal groundwaters in this semi-arid environment, it follows that a seasonal signal will be preserved in the $\delta^{18}\text{O}_{\text{calcite}}$ values of Soreq Cave speleothems.

The oxygen isotope data for previous Soreq Cave paleoclimate studies (Bar-Matthews et al., 1997, 2003) were acquired by acid-digestion of calcite powder drilled from speleothem samples using a 0.5–1.0 mm-diameter dental drill. Each drill-spot represents a finite period of time determined by the growth rate of the speleothem. In Soreq Cave, stalagmite growth rates are generally between ~ 0.01 and 0.1 mm yr^{-1} . This typically corresponds to a temporal resolution of 10–100 yr for each drill analysis, and where there are discontinuities in growth, individual analyses can integrate over a century of calcite precipitation.

The current study explores the paleoclimate record by combining imaging with high spatial-resolution and high-precision ion microprobe analysis in order to determine if an oxygen isotope record exists

* Corresponding author. Fax: +1 608 262 0693.

E-mail address: orland@geology.wisc.edu (I.J. Orland).

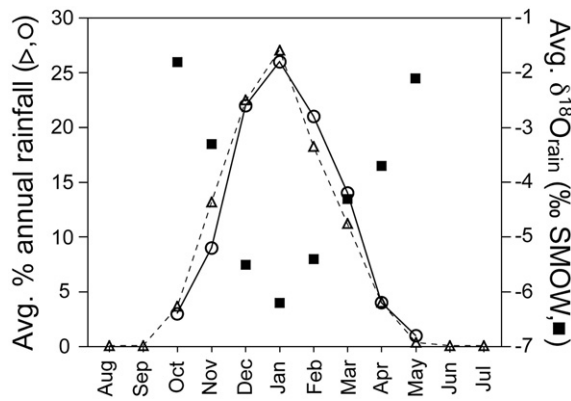


Figure 1. Modern rainfall data from the Eastern Mediterranean region. Open circles and triangles show the average percentage of total annual rainfall per month (left axis) from Ayalon et al. (2004) and Mitchell and Jones (2005), respectively. Data from Ayalon et al. (2004) were collected from above Soreq Cave. Data from Mitchell and Jones (2005) were acquired from the CRU TS 2.1 database and represent interpolated rainfall within ~500 km of Soreq Cave from 1901 to 2002. The filled squares illustrate the monthly average of rainfall $\delta^{18}O$ values (right axis) collected above Soreq Cave from 1995–2008.

in sub-annual detail. Although high spatial-resolution measurement of $\delta^{18}O_{calcite}$ values has been previously accomplished in speleothems using ion microprobes (Kolodny et al., 2003; Treble et al., 2005, 2007), these studies all report experimental difficulties affecting accuracy, and no studies of the pre-instrumental climate record have documented sub-annual growth as a record of seasonality. If such a record is found in Soreq Cave, will it indicate seasonal variations, and will such variations provide a more accurate long-term record of drought, or of annual precipitation?

Modern cave setting and climate

Soreq Cave is situated in the carbonate-dominated western flank of the Judean Hills in central Israel ($31^{\circ}45.35'N$, $35^{\circ}1.35'E$; Fig. 2). The cave formed in Cenomanian Weradim Formation dolomite and is currently ~400 m above sea level and 40 km inland from the Mediterranean Sea. The cave roof varies in thickness from <10 to >40 m and some 50% of the hillslope above the cave has a shallow soil cover, 5–40 cm thick. Mediterranean C3-type vegetation predominates (Danin, 1988). Mean annual air temperature above Soreq Cave is $20.3^{\circ}C$. When the cave was discovered in 1968 as a result of quarrying, average measured air temperature was constant (annually) at $20.0^{\circ}C$ in the cave and temperatures varied seasonally from 19.5 – $20.5^{\circ}C$ (Asaf, 1975). There is no known pre-1968 opening to the cave.

Rainfall and dripwater patterns

The Eastern Mediterranean Sea is the dominant source of precipitation in central Israel today (Gat and Carmi, 1987; Bar-Matthews et al., 2003; Bar-Matthews and Ayalon, 2004). Ayalon et al. (1998) show that $\delta^{18}O$ and δD values in modern rainwater follow the Mediterranean Meteoric Water Line (MMWL). McGarry et al. (2004) concluded that the Eastern Mediterranean has consistently been the moisture source for central Israel for at least the last 140 ka.

As shown in Figure 1, there is a seasonal pattern to the amount and $\delta^{18}O$ value of modern rainfall above Soreq Cave (Ayalon et al., 2004). Ayalon et al. (1998) showed that this pattern was reflected in Soreq Cave dripwaters. For their study, Ayalon et al. collected two categories of dripwaters: “slow drip” and “fast drip”. Slow dripwaters dripped at rates <2 ml/day, while fast dripwaters—occurring only during the wet season—dripped at >6 ml/min and started immediately following heavy rainfall events. The sample in this study was located in an area of the cave where fast dripwaters are common during the winter months.

The slow dripwaters are interpreted to approach the “baseline” composition of water in the unsaturated zone above the cave (Ayalon et al., 1998). Kaufman et al. (2003) used tritium observations to find that the oldest age of dripwaters in Soreq Cave is ~30 yr and all dripwaters contain a component of younger water. The two major hydrological components that supply the slow dripwater reservoir are: 1) rains at the beginning and end of each rainy season that have relatively high $\delta^{18}O$ values and saturate the finer pores in the upper vadose zone, and 2) more intense rainfall, which has relatively low $\delta^{18}O$ values, that occurs during the wet season. Fast dripwaters are fed by intense wet-season rains and are more directly connected to the surface by high-permeability and fractured bedrock conduits. Infiltration of low- $\delta^{18}O$, wet-season rains into the vadose zone is incomplete as some rainwater with very low- $\delta^{18}O$ values from heavy storms is lost as runoff. The $\delta^{18}O$ value of infiltration is also increased due to evapotranspiration at the surface.

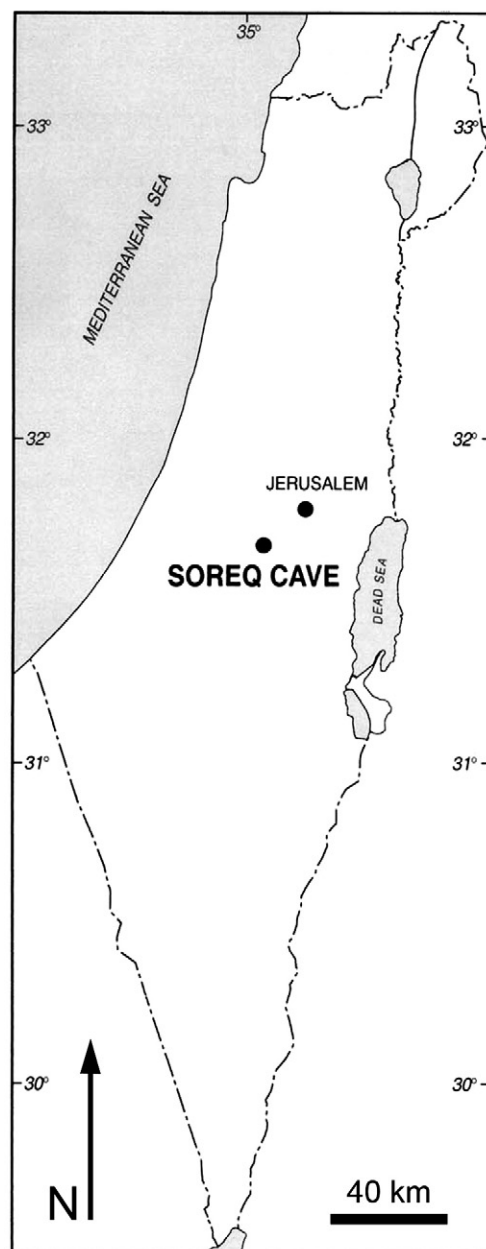


Figure 2. Map of Israel showing the location of Soreq Cave (adapted from Bar-Matthews et al., 2003).

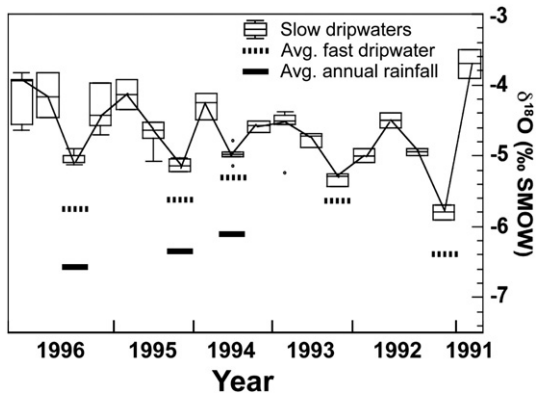


Figure 3. Values of $\delta^{18}\text{O}$ (SMOW) of modern dripwater from 1991–1996 in Soreq Cave. Values of “slow dripwater” are shown by open boxes, averaging 3–4 month intervals, and data from multiple drips show low variability. The annual variation in $\delta^{18}\text{O}$ values is typically $\sim 1\text{‰}$. “Fast dripwaters” (dashed lines) could only be collected during the peak of the wet season, and have consistently lower $\delta^{18}\text{O}$ values than concurrent slow dripwaters. The annual average $\delta^{18}\text{O}$ value of precipitation above the cave is shown by the heavy lines; the precipitation isotope value has a regular offset of $\sim 1\text{‰}$ from the $\delta^{18}\text{O}$ average fast dripwater values of that year. Cumulative measurements of annually averaged $\delta^{18}\text{O}_{\text{rain}}$ values before 1994 excluded some minor rainfall events and are not included here (adapted from Ayalon et al., 1998).

Between 1991 and 1996, slow dripwaters collected in Soreq Cave show a typical seasonal variation in $\delta^{18}\text{O}$ values of $\sim 1\text{‰}$ (Fig. 3). Fast dripwaters had $\delta^{18}\text{O}$ values that were $\sim 0.2\text{--}0.6\text{‰}$ lower than concomitant slow dripwaters, $\sim 1.0\text{--}1.5\text{‰}$ higher than the average $\delta^{18}\text{O}$ values of intensive rainstorms, and $\sim 0.3\text{--}1.0\text{‰}$ higher than the average of all rainfall events (Ayalon et al., 1998).

Effect of rainfall amount on $\delta^{18}\text{O}_{\text{rain}}$

The Eastern Mediterranean region today shows a strong seasonal contrast of winter and summer weather. Precipitation data collected between 1990 and 2007 from above Soreq Cave indicate that average annual rainfall is between 500 and 600 mm (Table A, Supplemental Materials). In general, 95% of the rainfall in this region occurs during the winter wet season, which extends from November until April. These rainfall records also show that values of $\delta^{18}\text{O}$ in precipitation are inversely correlated ($r^2=0.70$, $p<0.0001$) to annual rainfall amount by the equation:

$$\delta^{18}\text{O}_{\text{rain}}(\text{‰}, \text{VSMOW}) = -0.0036(\text{annual ppt, mm}) - 3.9 \quad (1)$$

Thus, an increase of $\delta^{18}\text{O}_{\text{rainfall}}$ values by 1‰ corresponds to ~ 280 mm less rain per year (Ayalon et al., 1998, 2004).

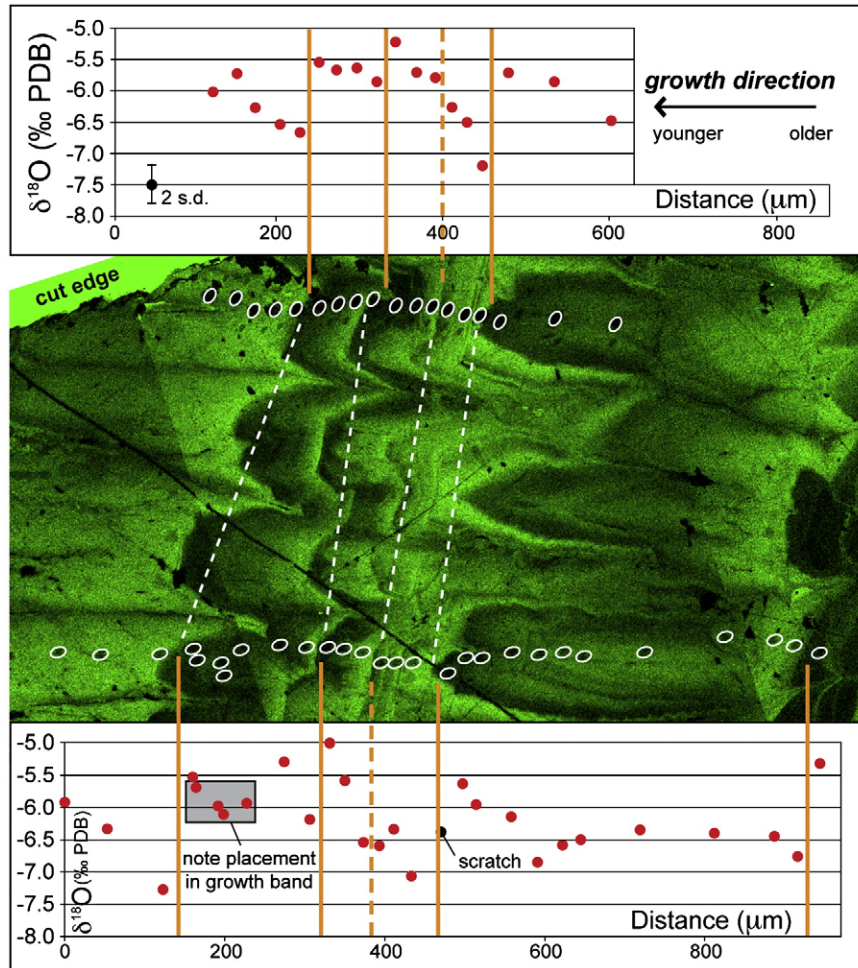


Figure 4. A fluorescent green image (true color) of sample 2-6 produced by confocal laser fluorescent microscopy for several annual light–dark couplets dated ca. 1.65 ka. Ion microprobe analysis spots, $10\ \mu\text{m}$ in diameter, are highlighted with white ovals. The horizontal axes of the two graphs are scaled to the fluorescent image in order to highlight the correlation of $\delta^{18}\text{O}$ (PDB) variation and growth bands. As a reference, the average spot-to-spot precision of these analyses ($2\ \text{s.d.} = \pm 0.32\text{‰}$) is plotted in the lower left of the upper graph. Values of $\delta^{18}\text{O}$ are lowest during the winter rainy season (bright fluorescence at the beginning of each band, marked by solid vertical lines) and gradually increase during the dry season as fluorescence darkens from right to left. The lower traverse was completed months after the upper traverse as a check of pattern reproducibility; the newer data may suggest the presence of an additional band, marked by the dashed vertical line in the graphs. Note that in the lower traverse, 1) a surface scratch compromised one analysis, and 2) the four highlighted analyses are in sequence with the saw-tooth pattern if their placement within the growth band is considered.

Surface, cave, and dripwater temperatures

The modern local climate at Soreq Cave is representative of Eastern Mediterranean semi-arid conditions. Average annual air temperature is 20.3°C; the wet-season average temperature is 14°C, while the dry season average is 26°C. Within Soreq Cave, air temperature varies by a maximum of ~2° (20–22°C). Measurements of dripwater temperature within the cave also vary annually by a maximum of ~2° (18–20°C) (Ayalon et al., 1998). Although special care, such as installing a double door, has been taken to maintain natural cave atmosphere conditions, these measured temperature fluctuations have likely been amplified by the presence of humans since the cave became a Nature Reserve in 1975. Therefore, it is reasonable to assume that 2°C is an upper bound on the annual temperature gradient of both the cave air and dripwater.

Also of note, Ayalon et al. (1998) observed a weak correlation ($r^2=0.42$, $p<0.0001$) between surface temperature and the $\delta^{18}\text{O}$ values of individual rain events in the vicinity of Soreq Cave. This relationship, which shows that increased surface temperatures correspond with increased $\delta^{18}\text{O}_{\text{rainfall}}$ values, reflects the seasonal variability shown in Figure 1.

With regard to the observed $\delta^{18}\text{O}_{\text{rain}}-T_{\text{surface}}$ relationship, it is important to evaluate the extent to which temperature, and specifically long-term temperature change, plays a role in controlling the isotope values measured in our speleothem sample. The empirical relationship of $\delta^{18}\text{O}_{\text{rain}}$ values and T_{surface} , which has a slope of ~1‰/2°C (see Fig. 4 in Ayalon et al., 1998), suggests a significant increase in average T_{surface} is needed to affect a large change in annually averaged $\delta^{18}\text{O}_{\text{dripwater}}$ values. Moreover, the temperature dependence of calcite–water equilibrium would work to diminish such an effect; a 2°C increase in cave and dripwater temperatures from 18 to 20°C will reduce the equilibrium $\delta^{18}\text{O}_{\text{calcite}}$ value by 0.45‰ (O’Neil et al., 1969). The combination of these two effects means that a hypothetical increase of 2°C in average T_{surface} might only increase the $\delta^{18}\text{O}_{\text{calcite}}$ value of speleothem growth by ~0.5‰. McGarry et al. (2004) calculated dripwater temperatures from $\delta^{18}\text{O}$ values of fluid inclusions in Soreq Cave speleothems and concluded that temperatures are constant over the last 1.3 ka. Although we have no direct, long-term record of surface temperatures in this region, it seems unlikely that average annual temperatures would have increased by 2°C (or more) on a centennial time scale in the late Holocene. Thus, for this study of a 2.2-ka-old speleothem we attribute changes in $\delta^{18}\text{O}_{\text{calcite}}$ values to the effect of rainfall amount.

Conditions of isotopic equilibrium

In order for $\delta^{18}\text{O}_{\text{calcite}}$ values of speleothems to be a reliable record of paleoprecipitation, the calcite needs to form under conditions of isotopic equilibrium in the cave. For this study, there are two processes that might confound interpretation of $\delta^{18}\text{O}_{\text{calcite}}$: 1) evaporation of groundwater in the vadose zone or 2) rapid degassing of CO_2 from dripwaters. First, the evaporation of vadose zone water has been evaluated at Soreq Cave by analysis of oxygen and hydrogen isotopes (Ayalon et al., 1998). Significant vadose zone evaporation would

increase both D/H and $^{18}\text{O}/^{16}\text{O}$ in groundwater, and would shift the dripwater compositions away from and below the MMWL. Values of $\delta^{18}\text{O}$ and δD from dripwater samples throughout the cave, however, plot along the MMWL indicating no significant (>1‰ in $\delta^{18}\text{O}$) evaporation. These results verify that the annual fluctuation of $\delta^{18}\text{O}_{\text{dripwater}}$ values in Soreq Cave is primarily due to the seasonal mixing of rainwater and water in the vadose seepage zone.

Second, some workers suggest that rapid outgassing of CO_2 from dripwater—a process that can cause non-equilibrium, kinetic fractionation of oxygen (and carbon) isotopes—is an important, and often overlooked, element of speleothem formation (Mickler et al., 2006). One way to test for disequilibrium processes is by comparing contemporaneous $\delta^{18}\text{O}$ records of multiple speleothems from the same cave. Dorale et al. (2002) called this the “replication test” and concluded that a positive correlation between such records strongly suggested that vadose zone and kinetic disequilibrium processes were not significant in that cave. Dorale et al. argued that by passing a replication test, a speleothem $\delta^{18}\text{O}$ record could be considered a primary environmental record. For this study, the inference of equilibrium conditions is based on the consistency of the composite $\delta^{18}\text{O}$ record of Soreq Cave speleothems (Bar-Matthews et al., 1997) and their correlation with foraminiferal $\delta^{18}\text{O}$ records from the adjacent Eastern Mediterranean Sea (Bar-Matthews et al., 2003).

Materials and methods

U–Th dating

This study examines Soreq Cave speleothem sample 2–6, a drip-formed stalagmite that is composed of low-magnesium calcite. The portion of the sample we examine here was cut perpendicular to the growth axis and has a radius of 5.5 cm. Eight U-series ages, obtained from MC-ICP-MS analyses at the Geological Survey of Israel (GSI), range from 2183 ± 170 to 1025 ± 110 yr (Table 1). Linear extrapolation of the average observed growth rate to the core and outer rim of the sample indicates that the speleothem grew from ~2.2–0.9 ka.

For each of the eight age measurements, ~0.3 g of calcite powder was dissolved in 7 N HNO_3 and a ^{236}U – ^{229}Th Harwell spike was added prior to U and Th purification. Each sample was loaded into minicolumns that contained 2 ml Bio-Rad AG 1 × 8 200–400 mesh resin. The U was eluted by 1 N HBr and Th with 6 N HCl. Afterwards, the U and Th solutions were dried and redissolved in 2 ml and 5 ml of 0.1 N HNO_3 , respectively.

Measurement of Th and U isotope ratios was performed at the GSI using a Nu Instruments Ltd. MC-ICP-MS equipped with 12 Faraday counters and 3 ion counters. The sample was loaded into the MC-ICP-MS through an Aridus® micro-concentric desolvating nebulizer sample introduction system. Instrumental mass bias was amended using an exponential equation by correcting the measured $^{238}\text{U}/^{235}\text{U}$ ratio to the known natural value. Calibration of ion counters relative to the Faraday cups was attained by cycling measurements through different collector configurations. The reproducibility of each measured $^{234}\text{U}/^{238}\text{U}$ ratio was 0.11% (2 σ) (Vaks et al., 2007).

Table 1
U/Th age data from MC-ICP-MS analysis of sample 2–6 from Soreq Cave

Sample	U conc. (ppm)	$^{234}\text{U}/^{238}\text{U}$	$^{230}\text{Th}/^{234}\text{U}$	$^{230}\text{Th}/^{232}\text{Th}$	Age (yr) uncorrected	Age (yr) corrected
2.6.1	0.5540 ± 0.0004	1.02931 ± 0.00145	0.01445 ± 0.00036	7.15 ± 0.18	1583 ± 80	1025 ± 110
2.6.2	0.5310 ± 0.0003	1.02859 ± 0.00099	0.01440 ± 0.00059	19.70 ± 0.81	1578 ± 130	1376 ± 150
2.6.3	0.5110 ± 0.0002	1.03124 ± 0.00081	0.01510 ± 0.00040	23.51 ± 0.62	1655 ± 90	1475 ± 105
2.6.4	0.5620 ± 0.0003	1.03288 ± 0.00087	0.01559 ± 0.00039	22.86 ± 0.47	1709 ± 90	1538 ± 105
2.6.5	0.4550 ± 0.0002	1.03359 ± 0.00120	0.01895 ± 0.00120	16.83 ± 1.08	2080 ± 260	1782 ± 310
2.6.6	0.4860 ± 0.0002	1.02976 ± 0.00249	0.01894 ± 0.00056	18.93 ± 0.56	2080 ± 120	1814 ± 145
2.6.7	0.4850 ± 0.0003	1.02791 ± 0.00165	0.01929 ± 0.00065	18.80 ± 0.63	2118 ± 140	1846 ± 170
2.6.8	0.5580 ± 0.0002	1.03047 ± 0.00134	0.02174 ± 0.00067	24.94 ± 0.78	2390 ± 150	2183 ± 170

The positions of age analyses in sample 2–6 are shown in Fig. 6. All errors are listed at the 2 σ confidence level.

Ages obtained from the U/Th ratios measured in Soreq Cave speleothems are corrected for detrital ^{232}Th (Table 1); the correction is based on an isochron method and is determined specifically for Soreq Cave speleothems (Kaufman et al., 1998). Kaufman et al. determine that the detrital components within Soreq Cave speleothems have a $^{232}\text{Th}/^{238}\text{U}$ ratio of ~ 1.8 .

Sample preparation, confocal laser fluorescent microscopy

After analysis for geochronology, a radial portion of sample 2–6 was cut into five ~ 1 -cm chips and mounted, along with 4–6 grains of UWC-3 (calcite standard; $\delta^{18}\text{O}=12.49\%$, VSMOW; Kozdon et al., in press), in three polished 2.5-cm-diameter epoxy rounds. At the University of Wisconsin-Madison (UW-Madison), we employed a number of analytical methods including secondary electron microscopy, backscatter electron microscopy, electron backscatter diffraction, and optical microscopy to determine that the sample was free of aragonite and any detrital material that might interfere with high spatial-resolution analysis.

Confocal laser fluorescent microscopy (CLFM) was subsequently completed at the Keck Bioimaging Laboratory at UW-Madison using a Bio-Rad MRC-1024 scanning confocal microscope operated with a 40-mW, 488-nm laser line. Images of speleothem fluorescence were collected using an emission filter that allows light with wavelengths between 505 and 539 nm (visible, green). Linear image adjustment was applied in order to increase the contrast and brightness of published images.

Ion microprobe analysis of $\delta^{18}\text{O}$

Ion microprobe oxygen isotope data were acquired at UW-Madison using a CAMECA ims-1280 large radius multicollector ion microprobe. A total of 719 oxygen analyses were made from ~ 10 - μm -diameter spots along a 5.5-cm traverse of sample 2–6. Spot sizes varied from 7–12 μm in diameter between the different analysis sessions depending on the primary beam condition. Throughout the experiment, 4–5 consecutive measurements of UWC-3 calcite standard were performed before and after every set of 10–15 sample analyses (Table B, Supplemental material). The ion microprobe instrumental mass fractionation factor ($\text{IMF}=\delta^{18}\text{O}_{\text{measured}}-\delta^{18}\text{O}_{\text{VSMOW}}$) in calcite is calculated from each bracketing set of eight or more measurements of UWC-3 and was typically -3.22% . The precision of a set of bracketing standard analyses, on average equal to 0.34% (2 standard deviations, s.d.; Table B, Supplemental material), was used to estimate the spot-to-spot reproducibility of a block of sample analyses; this value of reproducibility is the best estimate of the analytical uncertainty of individual sample analyses.

For each oxygen isotope analysis, we utilized a ~ 2.5 nA primary beam of $^{133}\text{Cs}^+$ ions, focused to ~ 10 μm in diameter at the sample surface, to sputter a 1- μm -deep pit in calcite. Charging of the sample surface was compensated by 1) an electron flood gun and 2) a gold coat on the epoxy mount, which was applied following cleaning in deionized water and ethyl alcohol. Each epoxy round was prepared such that all analytical spots were within 5 mm of the center of the mount and the UWC-3 standard. For the procedures used in the UW-Madison lab, this setup prevents instrument bias related to sample position such as reported by Treble et al. (2007).

A typical secondary $^{16}\text{O}^-$ ion intensity was 3×10^9 cps. The mass resolving power was 2200 and $^{18}\text{O}^-$ and $^{16}\text{O}^-$ ions were simultaneously collected by two Faraday Cup detectors in the multicollection system. Individual analyses took about 4 min each, which included pre-sputtering to burn through the Au coat (10 s), followed by automatic recentering of secondary ions in the field aperture (~ 60 s), and finally integration of oxygen ions for isotopic measurements (80 s; 20 cycles of 4-s integrations). More detailed analytical conditions are described by previous workers (Kelly et al., 2007; Kita et al., 2007; Page et al., 2007).

Results

Fluorescent banding

Confocal laser fluorescent microscopy (CLFM) of sample 2–6 reveals concentric banding (<1 μm to >100 μm in width) that occurs in a distinct cyclical pattern; the fluorescence of each band progresses gradually with time from “light” to “dark” with a sharp boundary to the next light fluorescent zone occurring at the end of each darkening gradient (Fig. 4). This sequence of fluorescence is observed across the entirety of the prepared sample. We use the terms “light” and “dark” to refer to fluorescent and non-fluorescent material, respectively, and not to isotope ratio for the remainder of this manuscript.

As shown by Figures 4 and 5, the width and gradient of the fluorescent pattern is different from one band to the next. Furthermore, there are a number of unconformities that truncate the bladed tips of older crystal growth; these truncations generally occur as straight bands of light calcite cutting across the dark portion of a bladed growth band. Truncations always “face” in the same direction (Fig. 5A). We count 182 bands thicker than 10 μm , and a further ~ 176 thinner than 10 μm , across this sample (growth spans ~ 1.3 ka). There are also “island” features where a single fluorescent band forms a continuous loop <200 μm in diameter (Fig. 5B); islands, which are uncommon in the radial section that we imaged, are probably the result of a calcite crystal growing with a different orientation on the outer surface of the speleothem.

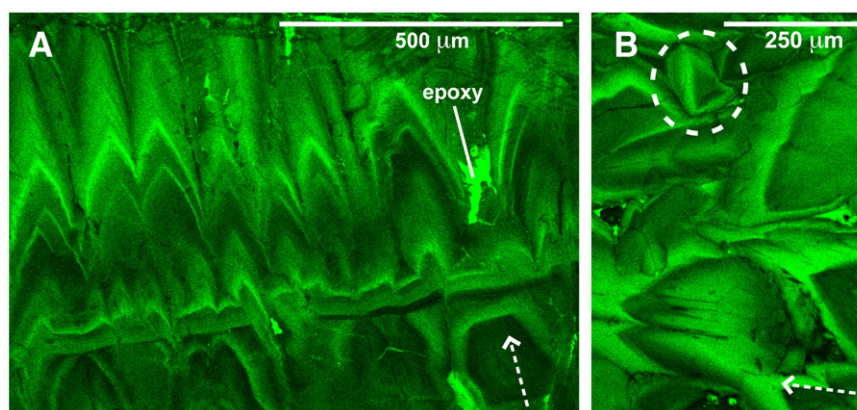


Figure 5. Confocal laser fluorescent microscopy images of interesting banding features in sample 2–6. Panel A shows a “truncation” feature that cuts across the regular, chevron banding pattern. The irregular fluorescent spot in panel A results from epoxy infilling porous space. Panel B highlights an “island” feature, uncommon in our sample, where a growth band appears to wrap around on itself; this feature is probably the result of a calcite crystal growing with a different orientation. The arrows in both panels indicate growth direction.

$\delta^{18}\text{O}$ analysesVariations of $\delta^{18}\text{O}$

The investigation of ion microprobe oxygen isotope compositions from sample 2–6 (Table B and Figs. A–E, Supplemental material) reveals a strong correlation between $\delta^{18}\text{O}$ values and the repeated pattern of light/dark fluorescent banding imaged by CLFM. Within single couplets that contain between 2 and 6 analyses, we observe consistently smooth increases of $\delta^{18}\text{O}$ values by as much as 2.15‰ from the light to the dark calcite (older to younger growth). Figure 4 illustrates this distinctive saw-tooth pattern through several cycles. Similar isotopic sequences are correlated to CLFM imaging throughout the sample.

On a broader scale, the 6-point running average of $\delta^{18}\text{O}_{\text{light calcite}}$ values (solid line in Fig. 6A) increases by $\sim 1\%$ between the oldest and youngest calcite in sample 2–6. The sharpest increase in this running average occurs at ca. 1.9 ka. We note that conventional drill-sample analysis across the entire sample 2–6 reveals a total variation in $\delta^{18}\text{O}_{\text{calcite}}$ values of 1.0‰; again, with the ion microprobe we observe variation of up to 2.15‰ in $\delta^{18}\text{O}$ values within a single growth band.

Variations of $\Delta^{18}\text{O}_{\text{dark-light}}$

The difference in $\delta^{18}\text{O}$ values, $\Delta^{18}\text{O}_{\text{dark-light}}$, between light and dark calcite of the same couplet (i.e., $\delta^{18}\text{O}_{\text{dark calcite}} - \delta^{18}\text{O}_{\text{light calcite}}$) varies

across the sample. Furthermore, the maximum values of $\Delta^{18}\text{O}_{\text{dark-light}}$ decrease from $>2.1\%$ to $<1.0\%$ between ~ 2.0 and 1.3 ka. This decrease in the isotopic contrast of individual growth bands is coincident with the increase in the running average of $\delta^{18}\text{O}_{\text{light calcite}}$ values (Fig. 6). Out of 75 bands analyzed across the sample, no dark calcite has a lower $\delta^{18}\text{O}$ value than its coupled light calcite (Fig. 6A).

Discussion

Annual fluorescent banding

There is contention surrounding the identification and utility of speleothem banding, annual or otherwise, in recent literature (Polyak and Asmerom, 2001; Betancourt et al., 2002; Baker and Genty, 2003; Asmerom and Polyak, 2004; Tan et al., 2006). The study of speleothem banding is still under development.

As described above, we used CLFM to detect and examine the regular fluorescent banding pattern. The combination of excitation and emission wavelengths (488 nm and 505–539 nm, respectively) employed to generate the fluorescence observed in sample 2–6 suggests that organic acids were present in dripwaters during calcite precipitation (Senesi et al., 1991; McGarry and Baker, 2000; Shopov, 2004). Tan et al. (2006) pointed to other studies in English and Chinese

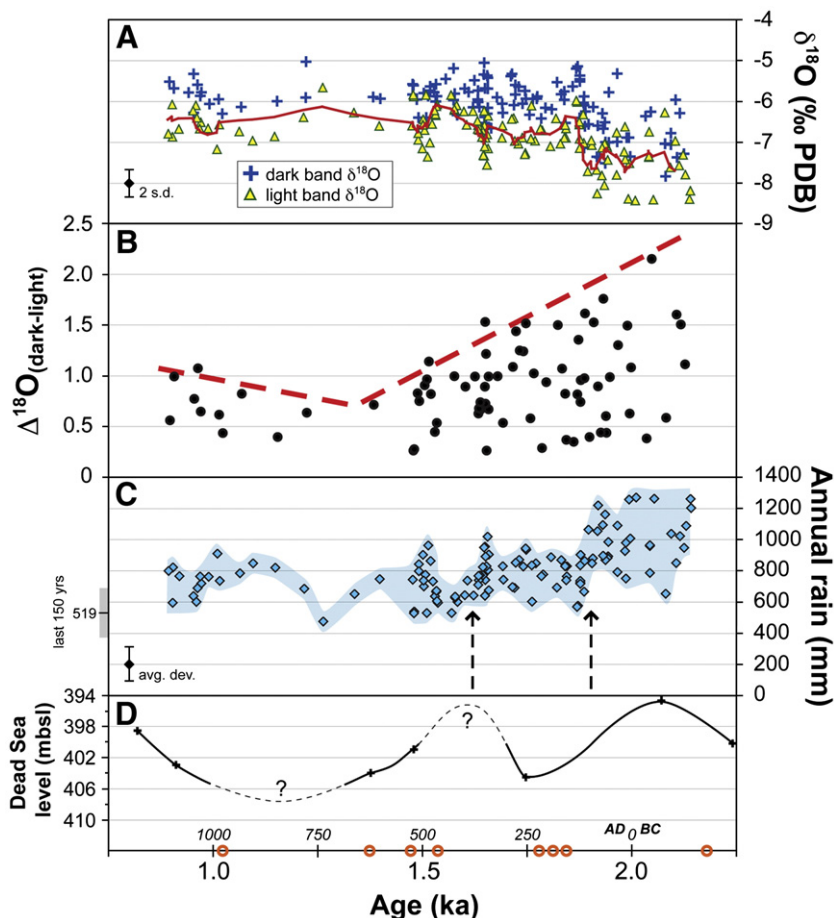


Figure 6. Panel A shows the measured $\delta^{18}\text{O}$ (PDB) values for ion microprobe analysis of light and dark fluorescent calcite bands across Soreq Cave sample 2–6. Analytical precision (2 s.d. = $\pm 0.34\%$) is illustrated in the lower left of panel A. For all 75 bands analyzed in this sample, the dark fluorescent calcite always has a higher $\delta^{18}\text{O}$ value than its coupled light fluorescent calcite. In general, for light fluorescent calcite, higher $\delta^{18}\text{O}$ values represent drier climates while lower $\delta^{18}\text{O}$ values are characteristic of wetter climates (see text for explanation). The heavy line, a 6-point running average, shows the general variability of $\delta^{18}\text{O}_{\text{light calcite}}$ values from 2.2–0.9 ka. Panel B shows values of $\Delta^{18}\text{O}_{\text{dark-light}}$ ($\delta^{18}\text{O}_{\text{dark calcite}} - \delta^{18}\text{O}_{\text{light calcite}}$) of individual annual bands. The heavy dashed line emphasizes the decrease in maximum $\Delta^{18}\text{O}_{\text{dark-light}}$ values from 2.0–1.3 ka. Panel C plots estimates of annual precipitation amounts (mm) calculated from the $\delta^{18}\text{O}$ values of wet-season calcite (light fluorescence) assuming a dripwater temperature of 19°C and Eq. (1); the dashed arrows highlight sharp decreases in annual rainfall amounts at ~ 1.9 and 1.6 ka. The shaded region represents the range of rainfall estimates calculated for dripwater temperature between 18 and 20°C . The average deviation of modern rainfall data from Eq. (1) is shown in the lower left of panel C. The mean and 1 s.d. range of annual rainfall in Jerusalem for the last 150 yr, as collected by the Israel Meteorological Survey, is plotted on the left axis. Panel D illustrates concurrent changes in another paleorainfall proxy for the Levant region, the Dead Sea level (mbsl; Bookman et al., 2004). The circles along the age-axis represent the eight U-series dates (ka) acquired by MC-ICP-MS (Table 1).

caves (Baker et al., 1993, 1999; Ban et al., 2005) that attribute similar patterns of fluorescence and banding caves to seasonal, climate-driven changes in the input of organic substances into cave dripwaters. Tan et al. concluded that climate regimes with distinct wet/dry seasons may produce an annual flush of organic acids from the soil column that is recorded in the light fluorescent growth banding of underlying speleothems; such a pattern, if observed in an appropriate climatic setting, likely represents annual banding.

Soreq Cave is ideally situated to record annual fluorescent bands. Not only are there distinct wet and dry seasons, but also the signal of annual climate variation is observed in the $\delta^{18}\text{O}$ values of dripwaters in the cave (Ayalon et al., 1998). Since groundwater mixing does not homogenize $\delta^{18}\text{O}_{\text{dripwater}}$ values in Soreq Cave, it follows that the signal of an annual flush of organic acids would be preserved. Thus, we suggest that in sample 2–6, the sharp onset of a fluorescent band is caused by increased rainfall at the beginning of the wet season. During the dry season, we hypothesize that decomposition of plant matter supplies organic acid to the upper soil column. Then, as rainfall returns to the region, organic acids are again flushed into the cave.

We should note that neither the intensity nor the persistence of the fluorescent signal within a band should be used as an indicator of a sub-annual timescale. Rather, we interpret these bands as delineating only the beginning/end of each annual wet/dry season cycle. The correlation of observed patterns of growth banding with sub-annual isotope measurements provides a test of the interpretation that the fluorescent bands in our sample record an annual cycle.

It should also be discussed that the total number of fluorescent bands counted (~358) is less than the number of years indicated by U-series geochronology (~1300). The record of some years is undoubtedly removed by truncations (Fig. 5A) or by periods of non-deposition. It is further uncertain whether some of the subtle changes in fluorescence represent discrete storm events or single years.

Oxygen isotope patterns and annual banding

The pattern of $\delta^{18}\text{O}$ variation described above and illustrated in Figure 4 bears a strong resemblance to the modern seasonal variation of $\delta^{18}\text{O}_{\text{dripwater}}$ values in Soreq Cave (Fig. 3) (Ayalon et al., 1998, 2004). Using this seasonal dripwater variation as a guide, we interpret the correlated patterns of $\delta^{18}\text{O}_{\text{calcite}}$ values and fluorescent banding as the annual cycle of wet and dry seasons prevalent in the region. The $\delta^{18}\text{O}$ values of light fluorescent portions reflect the low $\delta^{18}\text{O}$ values of mid-winter, wet-season rainfall. The gradual increase of $\delta^{18}\text{O}$ values across each band reflects an increased proportion of high- $\delta^{18}\text{O}$ vadose zone water, which we refer to here as “baseline” dripwater, contributing to dripwaters during warmer, drier months. Just as with the fluorescent banding, a sharp boundary occurs at the end of each gradient of increasing $\delta^{18}\text{O}$ values; the beginning of the following year's wet season, also marked by the flush of fluorescent organics, coincides with an abrupt drop of $\delta^{18}\text{O}_{\text{calcite}}$ values.

The $\delta^{18}\text{O}$ value of calcite at the beginning and end of each annual band is representative of dripwater from discrete periods of the seasonal cycle, the beginning of the winter wet season in November and spring/summer vadose zone water, respectively. Thus, $\Delta^{18}\text{O}_{\text{dark-light}}$ is a measure of “seasonality” and is obtained by analyzing the light and dark extremities of each resolvable band.

Prolonged wet periods are recorded by low $\delta^{18}\text{O}$ values, as seen ca. 2.0 ka in Figure 6A, and correlate with larger values of $\Delta^{18}\text{O}_{\text{dark-light}}$ in Figure 6B. Conversely, relatively dry periods, marked by higher $\delta^{18}\text{O}$ values after 1.9 ka, are characterized by decreasing maximum $\Delta^{18}\text{O}_{\text{dark-light}}$ values. Hence, the climatic transition that is inferred from the shift in $\delta^{18}\text{O}$ values is reflected in our measure of seasonality as the maximum value of $\Delta^{18}\text{O}_{\text{dark-light}}$ dropped from >2.1‰ to <1.0‰ between ~2.0 and 1.3 ka.

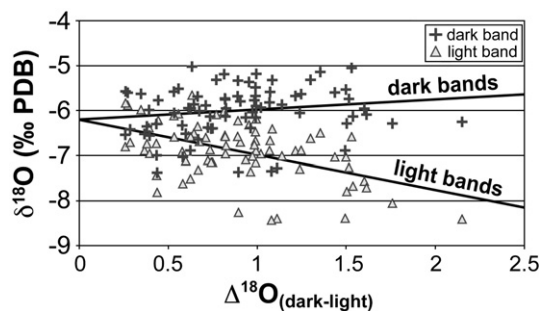


Figure 7. Measured $\delta^{18}\text{O}$ (PDB) values versus the $\Delta^{18}\text{O}_{\text{dark-light}}$ of each analyzed band in Soreq Cave sample 2–6. Dark fluorescent calcite $\delta^{18}\text{O}$ values (crosses) are relatively constant across the full range of observed $\Delta^{18}\text{O}_{\text{dark-light}}$ values, suggesting that the $\delta^{18}\text{O}$ of water in the vadose zone remained similar through time. Conversely, the $\delta^{18}\text{O}$ values of light fluorescent calcite (triangles) become more negative as $\Delta^{18}\text{O}_{\text{dark-light}}$ values increase. This trend is interpreted to reflect an increasing contribution of winter rains (see text for explanation).

Environmental interpretation of sub-annual isotope record from sample 2–6

Given our understanding of the modern hydrologic system above Soreq Cave, we propose a model that explains the empirical correlation between decreasing $\Delta^{18}\text{O}_{\text{dark-light}}$ values, the general drying of climate, and an increase in seasonal contrast (i.e., drier summers or shorter wet seasons). In our model, $\Delta^{18}\text{O}_{\text{dark-light}}$ values are driven by the proportionally larger contribution of wet-season rains to the low $\delta^{18}\text{O}$ values of light calcite. Figure 7 provides a test of this model; it illustrates that the $\delta^{18}\text{O}$ values of dark calcite, representative of the baseline vadose zone water, remain generally constant across the full range of $\Delta^{18}\text{O}_{\text{dark-light}}$ values observed in the sample. Although Figure 6A shows that the $\delta^{18}\text{O}$ values of dark calcite do shift across the sample, this change may reflect a response of the baseline vadose zone water to varying climate. Thus, the isotope composition of baseline vadose zone water remains relatively unchanged and $\Delta^{18}\text{O}_{\text{dark-light}}$ is determined by the amount that wet-season rains (that form light fluorescent calcite) depress the $\delta^{18}\text{O}$ value of groundwater supplied to the cave.

The model proposed above is consistent with the suggestion of Ayalon et al. (1998) that much of the precipitation at the beginning and end of each wet season must be sequestered in the porous upper vadose zone. By not immediately incorporating these short-lived, high- $\delta^{18}\text{O}$ -value rains directly into cave dripwaters, the sinusoidal pattern of $\delta^{18}\text{O}_{\text{rain}}$ variance (Fig. 1) is truncated into the saw-tooth pattern of $\delta^{18}\text{O}_{\text{calcite}}$ values observed in Figure 4. Similarly, Ayalon et al. (1998) observed that drip rates throughout the cave slow significantly during dry months; if too little water remains in the vadose zone to allow speleothems to grow during dry summers, the $\Delta^{18}\text{O}_{\text{dark-light}}$ signal would be correspondingly smaller.

Implications of a high-resolution speleothem record

The development of sub-annual resolution isotopic records in speleothems using *in situ* analysis by ion microprobe presents a number of avenues for additional paleoclimate and geochemical interpretations. First, by analyzing only the wet-season calcite—the light fluorescent portion of each band—it is possible to more accurately track significant changes in $\delta^{18}\text{O}_{\text{calcite}}$. As shown in Figure 7, the $\delta^{18}\text{O}$ values of light calcite in sample 2–6 are more representative of changing seasonality than the relatively constant $\delta^{18}\text{O}$ values of dark calcite. Furthermore, if the light portion of each growth band represents wet-season rainfall with a lesser component of baseline vadose zone water, then mixing of >30-yr-old (Ayalon et al., 1998; Kaufman et al., 2003) vadose zone water is avoided.

Second, by calculating $\delta^{18}\text{O}_{\text{groundwater}}$ values from the measured values of $\delta^{18}\text{O}$ in wet-season calcite (O'Neil et al., 1969), we can estimate paleorainfall amounts based on modern empirical data. Past studies (Ayalon et al., 1998; Bar-Matthews and Ayalon, 2004; Ayalon et al., 2004) show that at Soreq Cave: 1) $\delta^{18}\text{O}_{\text{average fast dripwater}} - \delta^{18}\text{O}_{\text{average rain}} = \sim 1\text{‰}$, and 2) there is a linear correlation between annual precipitation, in mm, and annual average $\delta^{18}\text{O}_{\text{rain}}$ given by Eq. (1). Using these relations, we suggest that the measured variation of $\delta^{18}\text{O}_{\text{calcite}}$ between 1.9 and 1.3 ka represents a decrease in average annual precipitation by as much as 300–400 mm (Fig. 6C). The record of paleorainfall in Figure 6C contrasts with previous studies from other Soreq Cave speleothems that could not resolve sub-annual variation (Bar-Matthews et al., 1998; Bar-Matthews and Ayalon, 2004). The calculated changes in paleorainfall estimates of earlier studies were smoothed because their isotope sampling methods mixed together both winter and summer calcite deposition from multiple years. With the ion microprobe we are able to measure $\delta^{18}\text{O}$ values of calcite deposited during single months or weeks of the wet season, thus resolving $\delta^{18}\text{O}$ values that are representative of the dominant rainwater compositions (light fluorescence, winter, fast dripwater) versus $\delta^{18}\text{O}$ that is influenced by vadose zone waters (dark fluorescence, spring/summer, slow dripwater).

It should be emphasized that these estimates of paleorainfall are based on three assumptions: 1) that the amount vs. $\delta^{18}\text{O}_{\text{rain}}$ relationship held over the time period during which the sample 2–6 grew, 2) that average annual temperature change was negligible across this time period, and 3) that average fast dripwater, represented by light fluorescent calcite, is consistently offset by 1‰ from the average $\delta^{18}\text{O}$ value of average annual rainfall. We think that all three assumptions are reasonable. With regard to the first assumption, the moisture source for this region has been the Mediterranean Sea for at least the last 140 ka (McGarry et al., 2004). Furthermore, the $\delta^{18}\text{O}$ value of the Mediterranean has been almost constant over the past 2.0 ka (Schilman et al., 2001). Thus, it is reasonable to think that the amount vs. $\delta^{18}\text{O}_{\text{rain}}$ relationship (Eq. (1)) held for the time interval represented by sample 2–6. The second assumption, that average annual temperature was constant across the period of growth, is supported by cave-air temperatures calculated from fluid inclusions (McGarry et al., 2004) and sea surface temperatures of the Eastern Mediterranean Sea (Emeis et al., 1998, 2000). The third assumption, that $\delta^{18}\text{O}_{\text{average fast dripwater}} - \delta^{18}\text{O}_{\text{average rain}} = \sim 1\text{‰}$, is based on empirical observations made by Bar-Matthews and Ayalon (2004).

The third implication of high-resolution isotopic studies of speleothems is the possibility for better understanding equilibrium and kinetic deposition processes. It is clear from the irregular banding pattern and the range of $\delta^{18}\text{O}$ values measured within single growth bands of sample 2–6 that one of the conventional tests of equilibrium deposition, the Hendy (1971) test, would return erroneous results with dental drill sampling. For sample 2–6, and probably many others, such a test would have to be carried out with an ion microprobe targeted with detailed imaging to ensure that the required isotope measurements do not represent a bulk average of multiple growth zones. Although we did not examine carbon isotopes for this report, an in-depth study of $\delta^{13}\text{C}$ values in sample 2–6 may reveal information about overlying vegetation, cave ventilation, and the process of equilibrium deposition.

Climate deterioration from 1.9–1.3 ka (AD 100–700)

The discussion above presents new data that suggests decreasing rainfall and thus climate deterioration from AD 100–700 in the Levant region. Other important independent evidence for changes in rainfall comes from lake levels in the Dead Sea (Neev and Emery, 1995). Enzel et al. (2003) established a quantitative link between modern precipitation and Dead Sea levels and confirmed the direct influence of regional climate on the hydrology of the Dead Sea

basin. Radiocarbon ages of organic remains in the adjacent Mount Sedom salt caves (Frumkin et al., 1991, 2001) and exposed sedimentary sequences (Bookman et al., 2004) suggest that Dead Sea levels dropped by at least 10–15 m between ~ 100 BC and AD 700 (Fig. 6D). These studies agree with the oxygen isotope record presented here that indicates desiccation of regional climate from AD 100–700.

Finally, we note that the changes we detect in seasonality from Soreq Cave correspond to a time period where historical records exist. Issar and Zohar (2004) outlined the history of the Roman and Byzantine Empires in the Eastern Mediterranean, and concluded that climate change contributed to the decline of their rule in the Levant. Beginning in the 3rd century AD, the coupled effects of attacks on the eastern and northern borders of the Roman Empire, anarchy in Rome, and the suggested climate change weakened the economic system. Eventually, Byzantine rule in the Levant succumbed to the rapidly growing Islamic empire at the Battle of Yarmouk in AD 636, perhaps pressured by the inability of the agricultural economy to fully adjust to the drier climate (Issar and Zohar, 2004).

Our data support the hypothesis that climate change played a role in the decline of Roman rule in the Levant by showing a gradual decrease in annual rainfall punctuated by steep drops at \sim AD 100 and 400 (Fig. 6C). Furthermore, the decline in $\Delta^{18}\text{O}_{\text{dark-light}}$ values (Fig. 6B) suggests that there were always dry years, but the number of wet periods, which might have aided high crop yields, decreased.

Conclusions

The combination of laser confocal microscopy with high-resolution and high-precision oxygen isotope analysis of a Soreq Cave speleothem reveals a sub-annual record of paleoclimate in the Eastern Mediterranean region. High-precision ion microprobe analyses (average 2 s.d. = $\pm 0.34\text{‰}$, $\sim 10\text{-}\mu\text{m}$ -diameter spot) show regular fluctuations in $\delta^{18}\text{O}$ values that correlate to fluorescent banding; this pattern is interpreted to be an annual record of seasonal variation in rainfall. This is the first report of seasonality in speleothems dating from before the instrumental record of climate. Using these data, we document changes in both seasonality and annual precipitation in the region from 2.2–0.9 ka. Our estimates of steep drops in precipitation coincide with both a drop of water levels in the Dead Sea and the decline of Roman rule in this region. The combination of confocal laser fluorescent imaging and high-resolution ion microprobe oxygen isotope analysis is a viable method for evaluating paleoclimate at sub-annual resolution in Soreq Cave and should prove useful in other cave localities.

Acknowledgments

We thank J. Quade and two anonymous reviewers for comments that greatly improved this manuscript; T. Ushikubo and B. Fu for help with ion microprobe analysis; B. Hess and J. Kern for assistance with sample preparation; M. Spicuzza, Z. Liu, A. Carlson, and J. Kutzbach for helpful discussions; L. Rodenkirch for guidance at the Keck Bioimaging Lab at UW-Madison; J. Fournelle for help with the SEM; and the Israel Nature and Parks Authority for access to Soreq Cave. Funding came from NSF (EAR04-40343), DOE (93ER14389), Israel Science Foundation (grant 910/05), the Comer Science and Education Foundation, as well as Sigma Xi and the Department of Geology and Geophysics at UW-Madison. Wisc-SIMS is partly supported by the NSF (EAR03-19230, EAR07-44079).

Appendix A. Supplementary data

Supplementary data associated with this article can be found, in the online version, at doi:10.1016/j.yqres.2008.08.005.

References

- Asaf, M., 1975. Karstic features in Soreq Cave. Unpublished MSc thesis, Tel Aviv University, 66 p.
- Asmerom, Y., Polyak, V.J., 2004. Comment on "A test of annual resolution in stalagmites using tree rings." *Quaternary Research* 61, 119–121.
- Ayalon, A., Bar-Matthews, M., Sass, E., 1998. Rainfall-recharge relationships within a karstic terrain in the Eastern Mediterranean semi-arid region, Israel: $\delta^{18}\text{O}$ characteristics. *Journal of Hydrology* 207, 18–31.
- Ayalon, A., Bar-Matthews, M., Kaufman, A., 1999. Petrography, strontium, barium and uranium concentrations, and strontium and uranium isotope ratios in speleothems as palaeoclimatic proxies: Soreq Cave, Israel. *The Holocene* 9, 715–722.
- Ayalon, A., Bar-Matthews, M., Schilman, B., 2004. Rainfall isotopic characteristics at various sites in Israel and the relationships with unsaturated zone water. In: Geological Survey of Israel Reports, GSI/16/04. The Ministry of National Infrastructures, Jerusalem.
- Baker, A., Smart, P.L., Edwards, R.L., Richards, D.A., 1993. Annual growth banding in a cave stalagmite. *Nature* 364, 518–520.
- Baker, A., Proctor, C.J., Barnes, W.L., 1999. Variations in stalagmite luminescence laminae structure at Poole's Cavern, England, AD 1910 to AD 1996: calibration of a paleoprecipitation proxy. *The Holocene* 9, 683–688.
- Baker, A., Genty, D., 2003. Comment on "A test of annual resolution in stalagmites using tree rings." *Quaternary Research* 59, 476–478.
- Ban, F., Pan, G., Wang, X., 2005. Timing and possible mechanism of organic substance formation in stalagmite laminae from Beijing Shihua Cave. *Quaternary Sciences* 25, 265–268.
- Bar-Matthews, M., Ayalon, A., Matthews, A., Sass, E., Halicz, L., 1996. Carbon and oxygen isotope study of the active water-carbonate system in a karstic Mediterranean cave: implications for paleoclimate research in semiarid regions. *Geochimica et Cosmochimica Acta* 60, 337–347.
- Bar-Matthews, M., Ayalon, A., Kaufman, A., 1997. Late Quaternary paleoclimate in the Eastern Mediterranean region from stable isotope analysis of speleothems at Soreq Cave, Israel. *Quaternary Research* 47, 155–168.
- Bar-Matthews, M., Ayalon, A., Kaufman, A., 1998. Middle to Late Holocene (6500 years period) paleoclimate in the Eastern Mediterranean region from stable isotopic composition of speleothems from Soreq Cave, Israel. In: Issar, A.S., Brown, N. (Eds.), *Water, Environment and Society in times of Climate Change*. Kluwer Academic Publishers, Boston, pp. 203–214.
- Bar-Matthews, M., Ayalon, A., Gilmour, M., Matthews, A., Hawkesworth, C.J., 2003. Sea-land oxygen isotopic relationships from planktonic foraminifera and speleothems in the Eastern Mediterranean region and their implication for paleorainfall during interglacial intervals. *Geochimica et Cosmochimica Acta* 67, 3181–3199.
- Bar-Matthews, M., Ayalon, A., 2004. Speleothems as paleoclimate indicators, a case study from Soreq Cave located in the Eastern Mediterranean region, Israel. In: Battarbee, R.W., Gasse, F., Stickley, C.E. (Eds.), *Past Climate Variability through Europe and Africa*. Springer, Dordrecht, The Netherlands, pp. 363–391.
- Betancourt, J.L., Grissino-Mayer, H.D., Salzer, M.W., Swetnam, T.W., 2002. A test of "annual resolution" in stalagmites using tree rings. *Quaternary Research* 58, 197–199.
- Bookman, R., Enzel, Y., Agnon, A., Stein, M., 2004. Late Holocene lake-levels of the Dead Sea. *Bulletin of the Geological Society of America* 116, 555–571.
- Danin, A., 1988. Flora and vegetation of Israel and adjacent areas. In: Tom-Tov, Y., Tchernov, E. (Eds.), *The Zoogeography of Israel*. Dr. W. Junk Publishers, Dordrecht, The Netherlands.
- Dorale, J.A., Edwards, R.L., Onac, B.F., 2002. Stable isotopes as environmental indicators in speleothems. In: Daoxian, Y., Cheng, Z. (Eds.), *Karst processes and the carbon cycle: Final report of ICGP379*. Geologic Publishing House, Beijing, China, pp. 107–120.
- Emeis, K.C., Schulz, H.M., Struck, U., Sakamoto, T., Doose, H., Erlenkeuser, H., Howell, M., Kroon, D., Paterne, M., 1998. Stable isotope and alkenone temperature records of sapropels from sites 964 and 967: constraining the physical environment of sapropel formation in the eastern Mediterranean Sea. In: Robertson, A.H.F., Emeis, K.C., Richter, C., Camerlenghi, A. (Eds.), *Proceedings of the Ocean Drilling Program, Scientific Results*, 160. Ocean Drilling Program, College Station, pp. 309–331.
- Emeis, K.C., Struck, U., Schulz, H.M., Rosenberg, R., Bernasconi, S., Erlenkeuser, H., Sakamoto, T., Martinez-Ruiz, F., 2000. Temperature and salinity variations of Mediterranean Sea surface waters over the last 16,000 years from records of planktonic stable oxygen isotopes and alkenone unsaturation ratios. *Palaeogeography, Palaeoclimatology, Palaeoecology* 158, 259–280.
- Enzel, Y., Bookman, R., Sharon, D., Gvirtzman, H., Dayan, U., Baruch, Z., Stein, M., 2003. Late Holocene climates of the Near East deduced from Dead Sea level variations and modern regional winter rainfall. *Quaternary Research* 60, 263–273.
- Frumkin, A., Magaritz, M., Carmi, I., Zak, I., 1991. The Holocene climatic record of the salt caves of Mount Sedom, Israel. *The Holocene* 1, 191–200.
- Frumkin, A., Kadan, G., Enzel, Y., Eyal, Y., 2001. Radiocarbon chronology of the Holocene Dead Sea: attempting a regional correlation. *Radiocarbon* 43, 1179–1189.
- Gat, J.R., Carmi, I., 1987. Effect of climate changes on the precipitation and isotopic composition of water in a climate transition zone: case of the eastern Mediterranean Sea area. *IAHS Spec. Publ.* 168, 513–523.
- Hendy, C.H., 1971. The isotopic geochemistry of speleothems — I. The calculation of the effects of different modes of formation on the isotopic composition of speleothems and their applicability as paleoclimate indicators. *Geochimica et Cosmochimica Acta* 35, 801–824.
- Issar, A.S., Zohar, M., 2004. *Climate Change: Environment and Civilization in the Middle East*. Springer-Verlag, Berlin.
- Kaufman, A., Wasserburg, G.J., Porcelli, D., Bar-Matthews, M., Ayalon, A., Halicz, L., 1998. U-Th isotope systematics from the Soreq Cave, Israel and climatic correlations. *Earth and Planetary Science Letters* 156, 141–155.
- Kaufman, A., Bar-Matthews, M., Ayalon, A., Carmi, I., 2003. The vadose flow above Soreq Cave, Israel: a tritium study of the cave waters. *Journal of Hydrology* 273, 155–163.
- Kelly, J.L., Fu, B., Kita, N.T., Valley, J.W., 2007. Optically continuous silcrete quartz cements of the St. Peter sandstone: high precision oxygen isotope analysis by ion microprobe. *Geochimica et Cosmochimica Acta* 71, 3812–3832.
- Kita, N.T., Ushikubo, T., Fu, B., Spicuzza, M.J., and Valley, J.W., 2007. Analytical developments on oxygen three isotope analyses using a new generation ion microprobe IMS-1280. *Lunar Planetary Science Conference Abstracts* 38, #1981.
- Kolodny, Y., Bar-Matthews, M., Ayalon, A., McKeegan, K.D., 2003. A high spatial resolution $\delta^{18}\text{O}$ profile of a speleothem using an ion-microprobe. *Chemical Geology* 197, 21–28.
- Kozdon, R., Ushikubo, T., Kita, N.T., Spicuzza, M.J., and Valley, J.W., in press. Intratest oxygen isotope variability in planktonic foraminifera: Real vs. apparent vital effects by ion microprobe. *Chemical Geology*.
- Matthews, A., Ayalon, A., Bar-Matthews, M., 2000. D/H ratios of fluid inclusions of Soreq cave Israel speleothems as a guide to the Eastern Mediterranean Meteoric Line relationships in the last 120 ky. *Chemical Geology* 166, 183–191.
- McGarry, S.F., Baker, A., 2000. Organic acid fluorescence: applications to speleothem palaeoenvironmental reconstruction. *Quaternary Science Reviews* 19, 1087–1101.
- McGarry, S., Bar-Matthews, M., Matthews, A., Vaks, A., Schilman, B., Ayalon, A., 2004. Constraints on hydrological and paleotemperature variations in the Eastern Mediterranean region in the last 140 ka given by the δD values of speleothem fluid inclusions. *Quaternary Science Reviews* 23, 919–934.
- Mickler, P.J., Stern, L.A., Banner, J.A., 2006. Large kinetic isotope effects in modern speleothems. *Geological Society of America Bulletin* 118, 65–81.
- Mitchell, T.D., Jones, P.D., 2005. An improved method of constructing a database of monthly climate observations and associated high-resolution grids. *International Journal of Climatology* 25, 693–712.
- Neev, D., Emery, K.O., 1995. *The Destruction of Sodom, Gomorrah, and Jericho: Geological, Climatological, and Archaeological background*. Oxford University Press, New York.
- O'Neil, J.R., Clayton, R.N., Mayeda, T.K., 1969. Oxygen fractionation in divalent metal carbonates. *Journal of Chemical Physics* 51, 5547–5558.
- Page, F.Z., Ushikubo, T., Kita, N.T., Riciputi, L.R., Valley, J.W., 2007. High-precision oxygen isotope analysis of picogram samples reveals 2- μm gradients and slow diffusion in zircon. *American Mineralogist* 92, 1772–1775.
- Polyak, V.J., Asmerom, Y., 2001. Late Holocene climate and cultural changes in the southwest United States. *Science* 294, 148–151.
- Schilman, B., Bar-Matthews, M., Almogi-Labin, A., Luz, B., 2001. Global climate instability reflected by Eastern Mediterranean marine records during the late Holocene. *Palaeogeography, Palaeoclimatology, Palaeoecology* 176, 157–176.
- Senesi, N., Miano, T.M., Provenzano, M.R., Brunetti, G., 1991. Characterisation, differentiation and classification of humic substances by fluorescence spectroscopy. *Soil Science* 152, 259–271.
- Shopov, Y.Y., 2004. Activators of luminescence in speleothems as source of major mistakes in interpretation of luminescent paleoclimatic records. *International Journal of Speleology* 33, 25–33.
- Tan, M., Baker, A., Genty, D., Smith, C., Esper, J., Cai, B., 2006. Applications of stalagmite laminae to paleoclimate reconstructions: comparison with dendrochronology/climatology. *Quaternary Science Reviews* 25, 2103–2117.
- Treble, P.C., Chappell, J., Gagan, M.K., McKeegan, K.D., Harrison, T.M., 2005. In situ measurement of seasonal $\delta^{18}\text{O}$ variations and analysis of isotopic trends in a modern speleothem from southwest Australia. *Earth and Planetary Science Letters* 233, 17–32.
- Treble, P.C., Schmitt, A.K., Edwards, R.L., McKeegan, K.D., Harrison, T.M., Grove, M., Chen, H., Wang, Y.J., 2007. High resolution SIMS $\delta^{18}\text{O}$ analyses of Hulu Cave speleothem at the time of Heinrich event 1. *Chemical Geology* 238, 197–212.
- Vaks, A., Bar-Matthews, M., Ayalon, A., Matthews, A., Halicz, L., Frumkin, A., 2007. Desert speleothems reveal climatic window for African exodus of early modern humans. *Geology* 35, 831–834.